AD-A166 416 ANALYSIS OF GRADIENT CHANGE THRESHOLDS IN THE DETECTION OF EDGES OF OBJEC. (U) ARMY ARMAMENT RESEARCH AND DEVELOPMENT CENTER WATERVLIET NY C.. C N SHEN ET AL. 1/1

UNCLASSIFIED FEB 86 ARCCB-TR-86007 SBI-AD-E440 317 F/G 17/5 NL

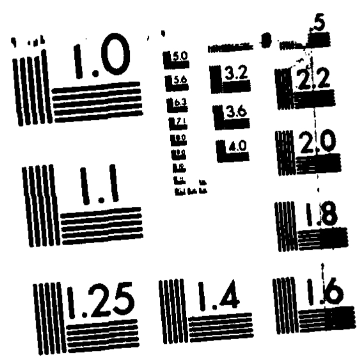

MICROCOPY RESOLUTION TEST CHART
NATIONAL BUREAU OF STANDARDS-1963-A

(13)

AD-A166 416

AD E440317

TECHNICAL REPORT ARCCB-TR-86007

ANALYSIS OF GRADIENT CHANGE THRESHOLDS IN THE DETECTION OF EDGES OF OBJECTS FROM RANGE DATA

C. N. SHEN

R. L. RACICOT

FEBRUARY 1986

US ARMY ARMAMENT RESEARCH AND DEVELOPMENT CENTER
CLOSE COMBAT ARMAMENTS CENTER
BENÉT WEAPONS LABORATORY
WATERVLIET, N.Y. 12189-4050

APPROVED FOR PUBLIC RELEASE; DISTRIBUTION UNLIMITED

SECURITY CLASSIFICATION OF THIS PAGE (When Data Entered)

REPORT DOCUMENTATION PAGE		READ INSTRUCTIONS BEFORE COMPLETING FORM
1. REPORT NUMBER ARCCB-TR-86007	2. GOVT ACCESSION NO. AD-A166 416	3. RECIPIENT'S CATALOG NUMBER
4. TITLE (and Subtitle) ANALYSIS OF GRADIENT CHANGE THRESHOLDS IN THE DETECTION OF EDGES OF OBJECTS FROM RANGE DATA		5. TYPE OF REPORT & PERIOD COVERED Final
		6. PERFORMING ORG. REPORT NUMBER
7. AUTHOR(s) C. N. Shen and R. L. Racicot		8. CONTRACT OR GRANT NUMBER(s)
9. PERFORMING ORGANIZATION NAME AND ADDRESS US Army Armament Research & Development Center Benet Weapons Laboratory, SMCAR-CCB-TL Watervliet, NY 12189-4050		10. PROGRAM ELEMENT, PROJECT, TASK AREA & WORK UNIT NUMBERS AMCMS No. 6111.01.91A0.011 PRON No. 1A52F59W1A1A
11. CONTROLLING OFFICE NAME AND ADDRESS US Army Armament Research & Development Center Close Combat Armaments Center Dover, NJ 07801-5001		12. REPORT DATE February 1986
		13. NUMBER OF PAGES 22
14. MONITORING AGENCY NAME & ADDRESS(if different from Controlling Office)		15. SECURITY CLASS. (of this report) UNCLASSIFIED
		15a. DECLASSIFICATION/DOWNGRADING SCHEDULE

16. DISTRIBUTION STATEMENT (of this Report)

Approved for public release; distribution unlimited.

17. DISTRIBUTION STATEMENT (of the abstract entered in Block 20, if different from Report)

18. SUPPLEMENTARY NOTES

Presented at the Third Army Conference on Applied Mathematics and Computing, Georgia Institute of Technology, Atlanta, Georgia, 13-16 May 1985.
Published in Proceedings of the Conference.

19. KEY WORDS (Continue on reverse side if necessary and identify by block number)

Gradient Change	Scanning Scheme
Detection	Laplacian Method
Threshold	Second Residual Method
Probabilities	

20. ABSTRACT (Continue on reverse side if necessary and identify by block number)

Edges of objects setting on or within a flat terrain can be defined by the slope or gradient change occurring at the edge. A simple estimate of slope change is to calculate the Laplacian using incremental range measurements taken at different elevation angles. The Laplacian is defined as the second difference of the range data. Since the range data contains noise in the form of measurement error, consideration must be given to the statistical aspects of

(CONT'D ON REVERSE)

DD FORM 1 JAN 73 1473 EDITION OF 1 NOV 65 IS OBSOLETE

UNCLASSIFIED

SECURITY CLASSIFICATION OF THIS PAGE (When Data Entered)

20. ABSTRACT (CONT'D)

detecting edges in order to differentiate between actual edges and noise effects. In this report, results are presented which describe the effects on minimum detectable slope change of (1) noise levels, (2) probability of miss, (3) probability of false alarm, (4) spacing of the measurements, and (5) random distribution of edges near range measurement points.

TABLE OF CONTENTS

	Page
INTRODUCTION	1
THE LAPLACIAN METHOD	1
THE RAPID ESTIMATION SCHEME AND COMPARISON OF ERROR PROBABILITIES	4
MINIMUM SLOPES OF DETECTABLE OBSTACLES	5
FUNCTION K OF ANGULAR GEOMETRY	7
THE SCANNING SCHEME	9
PROBABILITY OF DETECTION FOR RANDOMLY LOCATED EDGES	10
CONCLUSION	12
APPENDIX	20

TABLES

I.	FALSE ALARM PROBABILITIES AND MISS PROBABILITIES FOR VARIOUS $T/\sqrt{R}$ AND $u^*/\sqrt{R}$	3
II.	ERROR PROBABILITIES	4
III.	VALUES OF K AS FUNCTIONS OF GAMMA AND BETA + PHI	8
IV.	TOTAL PROBABILITY OF DETECTION FOR RANDOMLY LOCATED EDGES	13

LIST OF ILLUSTRATIONS

1.	Distributions and Probabilities Comparing the Two Methods.	15
2.	Obstacle Geometry.	15
3.	Angular Geometry.	16
4.	Projection Geometry.	17
5.	Scanning Factors.	18
6.	Reference Directions of Laser Rays Near an Edge Point.	19

INTRODUCTION

A laser range finder is installed on the top of a mast attached to a land vehicle or a helicopter. This laser range finder measures the distance between itself and the ground points on a terrain with obstacles. For segmentation, the edges of the boulder and crater must be estimated. In determining the near edges of a boulder or the far edges of a crater, it is necessary to locate the first differences of the slopes of the terrain. This is equivalent to finding the second differences of the terrain range points. The threshold values of the second differences can be in terms of an angle in a vertical plane. The probabilities of miss and false alarm can be ascertained depending on the method of estimation and the scanning scheme.

THE LAPLACIAN METHOD

The Laplacian Method considers cross-sections of terrain and looks for changes in slope in the azimuth or radial direction. Since we are only considering one-dimensional problems, we can write for the measurement equation

$$z_i = d_i + v_i \tag{1}$$

The change in slope is estimated by computing the following sufficient statistic:

$$s_i \overset{\Delta}{=} z_{i+1} - 2z_i + z_{i-1} \tag{2}$$

This is a digital approximation of the second derivative, or second difference, of the range.

Due to the presence of measurement noise in the calculation of s_i, it is impossible to discern with absolute certainty whether a change of slope

exists. The Neyman-Pearson criterion provides a decision rule which we may use to accurately detect edges of obstacles with a known probability of making an error. To produce the decision rule, first we must compute the variance of s_i as follows. We assume that the noise components v_i of the measurements are independent Gaussian random variables with zero mean and a variance of σ^2. Then, since z_{i+1}, z_i, and z_{i-1} are independent, Eqs. (1) and (2) yield

$$\begin{aligned} \mathrm{var}(s_i) &= \mathrm{var}(z_{i+1} - 2z_i + z_{i+1}) \\ &= \mathrm{var}(z_{i+1}) + \mathrm{var}(-2z_i) + \mathrm{var}(z_{i+1}) \\ &= \sigma^2 + 4\sigma^2 + \sigma^2 = 6\sigma^2 \end{aligned} \tag{3}$$

Because s_i is a scalar random variable, the Neyman-Pearson criterion provides a decision rule identical to that derived using hypothesis testing. The desired decision rule is

$$\mathrm{DECISION}_i = \begin{cases} \text{no signal} & \text{if } -T < s_i < T \\ \text{presence of signal} & \text{if } s_i \text{ is otherwise} \end{cases} \tag{4}$$

where T is the threshold in the decision process which can be determined from the equations

$$P_F = 2\phi[-T/\sqrt{6\sigma^2}] \tag{5}$$

$$P_M = \phi[(T-u^*)/\sqrt{6\sigma^2}] \tag{6}$$

where

$$\phi(z) = 1/\sqrt{2\pi} \int_{-\infty}^{z} e^{-\alpha^2/2}\, d\alpha \tag{7}$$

It is noted that the magnitude of s_i is not estimated by the Laplacian Method. The quantity u^* is called the "minimum detectable change of slope," since it is the smallest change of slope that can be detected with a miss probability of P_M or lower. The quantity P_F indicates the probability of a false alarm.

The miss probability P_M is the probability of not detecting a true change of slope equal to u*.

Typically, the standard deviation $\sqrt{R}$ is a known system parameter and u* is chosen so that suitable values of P_F and P_M can be obtained. Table I shows the trade-off of P_F vs. P_M for different values of the ratio $u^*/\sqrt{R}$. These values are computed using Eqs. (5) and (6).

TABLE I. FALSE ALARM PROBABILITIES AND MISS PROBABILITIES FOR VARIOUS $T/\sqrt{R}$ AND $u^*/\sqrt{R}$

$T/\sqrt{R}$	P_F	P_M For $u^*/\sqrt{R}=2$	P_M For $u^*/\sqrt{R}=3$	P_M For $u^*/\sqrt{R}=4$	P_M For $u^*/\sqrt{R}=5$	P_M For $u^*/\sqrt{R}=6$
1.000	.3174	.1587	.0227	.0013	.0000	.0000
1.500	.1336	.3085	.0668	.0062	.0002	.0000
1.679	.0932	.3741	.0932	.0102	.0005	.0000
2.000	.0456	.5000	.1587	.0227	.0013	.0000
2.146	.0319	.5580	.1966	.0319	.0022	.0001
2.500	.0124	.6915	.3085	.0668	.0062	.0002
3.000	.0026	.8413	.5000	.1587	.0227	.0013
3.500	.0003	.9332	.6915	.3085	.0668	.0062
4.000	.0000	.9772	.8413	.5000	.1587	.0227

THE RAPID ESTIMATION SCHEME AND COMPARISON OF ERROR PROBABILITIES

The variance of s_1 for the Laplacian Method is usually too high when a change of slope occurs during scanning. An adaptive method called Rapid Estimation Scheme is used instead to keep the variance lower, thus also reducing the probabilities of false alarm and miss. A discussion of the Second Residual Method for the Rapid Estimation Scheme is given in the Appendix.

The different expressions for the error probabilities of the two methods are given in Eqs. (5) and (6) and reiterated in Table II. We see that the expressions for both methods are the same except that $\sqrt{6\sigma^2}$ appears with the Laplacian Method, whereas $\sqrt{S_{1+2}}$ appears with the Second Residual Method.

TABLE II. ERROR PROBABILITIES

Method	Probability of False Alarm	Probability of Miss
Laplacian	$P_F^L = 2\phi[-T/\sqrt{6\sigma^2}]$	$P_M^L = \phi[(T-u^*)/\sqrt{6\sigma^2}]$
Second Residual	$P_F^S = 2\phi[-T/\sqrt{S_{1+2}}]$	$P_M^S = \phi[(T-u^*)/\sqrt{S_{1+2}}]$

We know that the Second Residual variance is less than or equal to the Laplacian variance:

$$\sqrt{S_{1+2}} \leq \sqrt{6\sigma^2} \tag{8}$$

Since $\phi(z)$ is a monotonically increasing function and has a negative argument in all the expressions in Table II (we assume $T-u^* < 0$), we can conclude that

$$P_F^S \text{ (Second Residual)} \leq P_F^L \text{ (Laplacian)} \tag{9}$$

$$P_M^S \text{ (Second Residual)} < P_M^L \text{ (Laplacian)} \tag{10}$$

Figure 1 illustrates how the smaller Second Residual variance leads to smaller error probabilities.

With smaller error probabilities, we expect the Second Residual Method will have a better performance over the Laplacian Method.

MINIMUM SLOPES OF DETECTABLE OBSTACLES

In this section we will determine the threshold in edging of gradient changes of obstacles. These may be detected using the Second Residual or the Laplacian Method.

Obstacles may or may not be detectable depending on the change of slopes of the terrain at its edges. It will be shown here that the minimum detectable slope change depends upon a given group of parameters.

Figure 2 shows a diagram of an obstacle. C and B are consecutive points where laser beams emanating from laser range finder bounce off the terrain. The slope of the obstacle is tan θ, since the slope between C and B is zero. The mast height is b, the height at which the laser range finder is located. Point D is the estimate of the range based on the data at point B and previous points. Thus, the range of point C is measured as z_{i+2} and point D lies at a range of $\bar{d}_{i+2}$, where $\bar{d}_{i+2} = HF_{i+1}x^*{}_{i+1}$ is the prediction of the range d_{i+2} from previous data. We see that the distance from C to D is the residue, r_{i+2}. It is apparent that the expected value of r_{i+2} takes its minimum value, u^*. From the geometry, the quantity tan θ can be computed by finding x/y. These quantities are found as follows:

$$x = u^* \sin \beta \tag{11}$$

$$y = \Delta\rho - u^* \cos \beta \tag{12}$$

then

$$\tan \theta = x/y = (u^* \sin \beta)/(\Delta\rho - u^* \cos \beta) \tag{13}$$

By extending the above idea, we have two slopes, AB and BC, instead of one in the previous cases as shown in Figure 3. The angle γ is the difference of the angle θ for slope BA and the angle ϕ for slope CB. Now the slope of γ becomes

$$\tan \gamma = \frac{a}{b} \quad , \quad (\gamma = \theta - \phi) \tag{14}$$

where

$$a = u^* \sin (\beta + \phi) \tag{15}$$

and

$$b = (\Delta\rho) \cos \phi - (\Delta\rho) \sin \phi \cot (\beta + \phi) - u^* \cos (\beta + \phi)$$

$$= (\Delta\rho) \frac{\sin (\beta+\phi) \cos \phi - \cos (\beta+\phi) \sin \phi}{\sin (\beta+\phi)} - u^* \cos (\beta+\phi)$$

$$= \frac{(\Delta\rho) \sin \beta}{\sin (\beta+\phi)} - u^* \cos (\beta+\phi)$$

$$= (\Delta\rho) \sin \beta \sin (\beta+\phi) \left[\frac{1}{\sin^2 (\beta+\phi)} - \frac{u^*}{(\Delta\rho) \sin \beta} \frac{1}{\tan (\beta+\phi)}\right] \tag{16}$$

Combining the terms, we have

$$\tan \gamma = \frac{(u^*/\tau) \tan^2 (\beta+\phi)}{1 + \tan^2 (\beta+\phi) - (u^*/\tau) \tan (\beta+\phi)} \tag{17}$$

where

$$\tau = (\Delta\rho) \sin \beta \tag{18}$$

The quantity τ is the projection of the data spacing in the direction of sin β.

If Eq. (17) is solved for u^*/τ, we have

$$u^*/\tau = K(\gamma,\beta+\phi) \overset{\Delta}{=} \frac{\tan\gamma\,[1 + \tan^2(\beta+\phi)]}{\tan(\beta+\phi)\,[\tan(\beta+\phi) + \tan\gamma]} \tag{19}$$

Table III gives the values of K as a function of angle of detection γ and the sum of the elevation angle β and the terrain angle ϕ, $(\beta+\phi)$.

The above equation can also be derived from Figure 4 which gives

$$u^*/\tau = K(\gamma,\beta+\phi) \overset{\Delta}{=} [\cot(\beta+\phi) - \cot(\beta+\phi+\gamma)] \tag{20}$$

FUNCTION K OF ANGULAR GEOMETRY

If we can keep the ratio u^*/τ constant in Eq. (19) or (20), then the value of $K(\gamma,\beta+\phi)$ will be constant in Table III. This can be achieved by letting both $u^*/\sqrt{R}$ and $\tau/\sqrt{R}$ be constant. First, we will discuss the value of $u^*/\sqrt{R}$.

Table I shows the values of P_F for given threshold to noise ratio $T/\sqrt{R}$ which guarantees the probability of detection. It also lists the values of P_M for both $T/\sqrt{R}$ and the signal to noise ratio, $u^*/\sqrt{R}$. For example, let us take $T/\sqrt{R} = 1.679$ and $u^*/\sqrt{R} = 3$. We have

$$P_F = 0.0932 \tag{21a}$$

$$P_M = 0.0932 \tag{21b}$$

which are reasonable values for our problem.

The second part is to keep the ratio $\tau/\sqrt{R}$ constant. This is related to the scanning scheme given in the next section. From Eq. (18), we have

$$\tau/\sqrt{R} = (\Delta\rho)(\sin\beta)/\sqrt{R} = \text{constant} = L \tag{22}$$

Then the ratios

$$\frac{u^*/\sqrt{R}}{\tau/\sqrt{R}} = \frac{3}{L} = K(\gamma,\beta+\phi) \tag{23}$$

TABLE III. VALUES OF K AS FUNCTIONS OF GAMMA AND BETA + PHI

Gamma	Beta + Phi 5	10	15	20	25	30	35	40	45	50
0	0.0	0.0	0.0	0.0	0.0	0.0	0.0	0.0	0.0	0.0
2	3.2857	0.9667	0.4612	0.2724	0.1819	0.1317	0.1011	0.0811	0.0675	0.0578
4	5.1163	1.6605	0.8278	0.5014	0.3405	0.2495	0.1933	0.1562	0.1307	0.1126
6	6.2855	2.1839	1.1270	0.6972	0.4802	0.3557	0.2778	0.2261	0.1902	0.1646
8	7.0986	2.5936	1.3762	0.8668	0.6046	0.4521	0.3558	0.2913	0.2464	0.2142
10	7.6980	2.9238	1.5875	1.0154	0.7164	0.5403	0.4281	0.3527	0.2998	0.2617
12	8.1592	3.1962	1.7694	1.1471	0.8175	0.6214	0.4956	0.4105	0.3506	0.3074
14	8.5258	3.4252	1.9280	1.2649	0.9096	0.6965	0.5589	0.4652	0.3991	0.3514
16	8.8250	3.6210	2.0678	1.3711	0.9941	0.7664	0.6184	0.5172	0.4457	0.3939
18	9.0742	3.7906	2.1922	1.4675	1.0721	0.8316	0.6746	0.5669	0.4905	0.4351
20	9.2856	3.9392	2.3039	1.5557	1.1445	0.8930	0.7279	0.6144	0.5337	0.4751
22	9.4674	4.0709	2.4050	1.6369	1.2120	0.9508	0.7787	0.6600	0.5755	0.5142
24	9.6260	4.1887	2.4972	1.7119	1.2752	1.0055	0.8273	0.7040	0.6161	0.5524
26	9.7658	4.2949	2.5817	1.7818	1.3347	1.0575	0.8738	0.7465	0.6557	0.5898
28	9.8902	4.3913	2.6597	1.8471	1.3910	1.1072	0.9186	0.7877	0.6943	0.6265
30	10.0019	4.4795	2.7321	1.9084	1.4443	1.1547	0.9618	0.8278	0.7321	0.6628
32	10.1030	4.5607	2.7995	1.9662	1.4951	1.2003	1.0037	0.8668	0.7691	0.6986
34	10.1952	4.6357	2.8628	2.0209	1.5436	1.2443	1.0443	0.9050	0.8056	0.7340
36	10.2797	4.7056	2.9223	2.0730	1.5902	1.2868	1.0838	0.9424	0.8416	0.7692
38	10.3577	4.7709	2.9785	2.1226	1.6350	1.3280	1.1224	0.9792	0.8772	0.8042
40	10.4301	4.8322	3.0318	2.1701	1.6782	1.3681	1.1602	1.0154	0.9125	0.8391
42	10.4795	4.8900	3.0826	2.2158	1.7200	1.4071	1.1973	1.0512	0.9476	0.8740
44	10.5608	4.9447	3.1312	2.2597	1.7606	1.4453	1.2338	1.0866	0.9825	0.9090
46	10.6203	4.9968	3.1777	2.3022	1.8002	1.4827	1.2698	1.1218	1.0175	0.9442
48	10.6765	5.0464	3.2225	2.3435	1.8388	1.5195	1.3054	1.1568	1.0524	0.9796
50	10.7299	5.0939	3.2657	2.3835	1.8766	1.5557	1.3407	1.1918	1.0875	1.0154
52	10.7807	5.1396	3.3076	2.4226	1.9136	1.5915	1.3757	1.2267	1.1228	1.0517
54	10.8292	5.1835	3.3482	2.4607	1.9501	1.6269	1.4107	1.2617	1.1584	1.0884
56	10.8758	5.2261	3.3877	2.4981	1.9861	1.6621	1.4456	1.2969	1.1944	1.1258
58	10.9205	5.2673	3.4263	2.5349	2.0217	1.6971	1.4806	1.3323	1.2309	1.1640
60	10.9638	5.3073	3.4641	2.5711	2.0570	1.7321	1.5156	1.3681	1.2679	1.2031

If L is chosen as 4, then one will look at the points for K = 0.75 in Table III. If L is chosen as 1.6, then one will look at the points for K = 1.875 in Table III. For K = 0.75, the following set of angles appears:

$\beta+\phi$	15°	20°	25°	30°
γ	3.8°	6.7°	10.2°	15.8°

In summary, the above value of γ is guaranteed to be detected for the conditions

$$u^*/\sqrt{R} = 3 \quad , \quad P_F = P_M = 0.0932 \quad , \quad \tau/\sqrt{R} = 4$$

and the variable $\beta+\phi$ as listed.

THE SCANNING SCHEME

In order for the value of L to be constant in Eq. (22), one will take the discrete form in Figure 5 as

$$(\Delta\rho)_1 \sin \beta_1 = (\Delta\rho)_2 \sin \beta_2 = \tau = \sqrt{R}\, L = \text{constant} \tag{23}$$

If b is the height of the mast, then

$$\sin \beta_1 = \frac{b}{\sqrt{b^2+\rho_1{}^2}} \qquad \sin \beta_2 = \frac{b}{\sqrt{b^2+\rho_2{}^2}} \tag{24}$$

Thus, we have in Figure 4

$$\frac{(\Delta\rho)_1}{\sqrt{b^2+\rho_1{}^2}} = \frac{(\Delta\rho)_2}{\sqrt{b^2+\rho_2{}^2}} = \frac{\tau}{b} = \frac{\sqrt{R}L}{b} \tag{25}$$

The above equation indicates that the spacing of the horizontal projection is proportional to the radial distances from the laser to points on the horizontal plane. For example, let us take b = 2, then

$$\frac{(\Delta\rho)_1}{\sqrt{4+\rho_1{}^2}} = \frac{(\Delta\rho)_2}{\sqrt{4+\rho_2{}^2}} = \frac{\sqrt{R}L}{2} \tag{26}$$

or

$$(\Delta\rho)_i = (\sqrt{4+\rho_i^2})\sqrt{R}L/2 \tag{26}$$

For example, given $\sqrt{R} = 0.125$ and $L = 1.6$ or $\sqrt{R} = 0.05$ and $L = 4.0$, in both cases we have $\tau = \sqrt{R}L = 0.20$. Then, from Eq. (26), we have

ρ	2 m	5 m	10 m	20 m
$\Delta\rho$	0.2828 m	0.5353 m	1.1832 m	2.010 m

In this case we may miss a boulder of 0.2 m at 2 m away or a boulder of 2 m at 20 m away.

PROBABILITY OF DETECTION FOR RANDOMLY LOCATED EDGES

In the previous sections it was assumed that range measurements were available from the range finder to the exact vertex of an edge. This is represented by point B in Figures 2 and 3. An edge is defined here by a discrete angular change γ. If the range measurement falls exactly on an edge, then only a deterministic value for the residue u^* in Eq. (19) is obtained. This, in turn, corresponds to a deterministic value for the P_D, probability of detection, in which $P_D = 1-P_M$ with P_M being given by Eq. (6).

In practice, however, the edges of objects might be randomly distributed and the range measurements, in general, might not fall exactly on an edge. A more realisitc approach, therefore, might be to treat the range measurements to be randomly distributed near an edge represented, for example, by points $\bar{A}$, $\bar{B}$, and $\bar{C}$ in Figure 6. A random residual $\bar{u}^*$ would result for given edge angular change γ instead of the constant deterministic value of u^* assumed previously.

The probability of detection in this case can be calculated using Eq. (6) as a function of the random variable $\bar{u}^*$:

$$P(\text{Detection}|\bar{u}^*) = 1 - P\,(\text{Miss}|\bar{u}^*) = 1 - \Phi\left[\frac{T-\bar{u}^*}{\sqrt{R}}\right] \tag{27}$$

From geometric considerations, it can be shown that $\bar{u}^*$ will range approximately from $u^*/2$ to u^* in Figure 6. It can be further assumed that the distribution of $\bar{u}^*$ will be uniform over this range of values which corresponds to a purely random distribution of object edges on a given terrain. Equation (27) can then be used to determine the total probability of detection:

$$P(\text{Detection}) = \int_{u^*/2}^{u^*} P(\text{Det}|\bar{u}^*)f(\bar{u}^*)d\bar{u}^*$$

$$= \frac{2}{u^*}\int_{u^*/2}^{u^*} P(\text{Det}|\bar{u}^*)d\bar{u}^*$$

$$= \frac{2}{u^*}\int_{u^*/2}^{u^*} \left(1-\Phi\left[\frac{T-\bar{u}^*}{\sqrt{R}}\right]\right)d\bar{u}^* \tag{28}$$

in which $f(\bar{u}^*)$ equals uniform distribution on ($u^*/2$ to u^*), and u^* is given by Eq. (19).

Equation (28) can be solved as a function of T, $\sqrt{R}$, and u^* where u^* is a function of γ, $(\beta+\phi)$, and τ as in Eq. (19). As an example, let

$T/\sqrt{R}$ = threshold level for detection

= 2.146; gives $P_F = 0.0319$ from Table I

$\sqrt{R}$ = $\sqrt{6\sigma^2}$ where σ = range data noise level

= 0.1225 for $\sigma = 0.05$

τ = 0.20

The resulting P(Detection) is shown in Table IV as a function of the angle change γ and $(\beta+\phi)$. Other similar information can readily be generated for other parameter values depending on the actual problem to be solved.

The behavior of the minimum detectable angular change γ can be readily determined from the type of information given in Table IV. For example, by requiring P(Detection) = 0.90 and letting $\beta+\phi = 15$ degrees, results in a minimum detectable value of γ to be about 40 degrees. This compares to a value of γ at 13 degrees for the nonrandom case previously considered where the range is assumed to be measured directly to the edge vertex.

CONCLUSION

For an assigned probability of false alarm and miss, one can determine the signal to noise ratio and the threshold to noise ratio. If we use a special scanning scheme such that the spacing of horizontal projections is proportional to the radial distances from the laser to a horizontal plane, then the function K of angular geometry is also constant. The detectable angle γ with certain probability can be found if K and $\beta+\phi$ are known. The angles $\beta+\phi$ are related to the elevation angle β and the terrain slope ϕ.

The following results were discussed in this report:

1. Ability to detect the change of slopes in a terrain for navigation of vehicles or robotic platforms.

2. Determination of the probability of false alarm and the probability of detection for various signal to noise ratios and for the case of randomly distributed measurements.

TABLE IV. TOTAL PROBABILITY OF DETECTION FOR RANDOMLY LOCATED EDGES

Gamma	2	4	6	8	10	Beta + Phi 12	14	16	18	20
0	0.0	0.0	0.0	0.0	0.0	0.0	0.0	0.0	0.0	0.0
2	1.0000	0.9960	0.7526	0.3606	0.1741	0.1004	0.0676	0.0508	0.0412	0.0352
4	1.0000	1.0000	0.9730	0.7563	0.4583	0.2645	0.1636	0.1110	0.0816	0.0641
6	1.0000	1.0000	0.9962	0.9077	0.6794	0.4431	0.2831	0.1891	0.1343	0.1011
8	1.0000	1.0000	0.9993	0.9605	0.8079	0.5895	0.4016	0.2742	0.1941	0.1440
10	1.0000	1.0000	0.9998	0.9812	0.8790	0.6960	0.5055	0.3575	0.2565	0.1901
12	1.0000	1.0000	1.0000	0.9902	0.9199	0.7707	0.5909	0.4338	0.3176	0.2372
14	1.0000	1.0000	1.0000	0.9944	0.9445	0.8230	0.6592	0.5013	0.3754	0.2838
16	1.0000	1.0000	1.0000	0.9967	0.9600	0.8603	0.7133	0.5595	0.4286	0.3286
18	1.0000	1.0000	1.0000	0.9979	0.9703	0.8874	0.7562	0.6094	0.4768	0.3710
20	1.0000	1.0000	1.0000	0.9986	0.9774	0.9076	0.7905	0.6519	0.5202	0.4107
22	1.0000	1.0000	1.0000	0.9990	0.9823	0.9230	0.8181	0.6881	0.5590	0.4476
24	1.0000	1.0000	1.0000	0.9993	0.9859	0.9350	0.8407	0.7191	0.5937	0.4817
26	1.0000	1.0000	1.0000	0.9995	0.9886	0.9444	0.8593	0.7457	0.6245	0.5131
28	1.0000	1.0000	1.0000	0.9996	0.9906	0.9520	0.8748	0.7687	0.6522	0.5421
30	1.0000	1.0000	1.0000	0.9997	0.9922	0.9582	0.8879	0.7887	0.6770	0.5687
32	1.0000	1.0000	1.0000	0.9998	0.9934	0.9632	0.8990	0.8062	0.6993	0.5933
34	1.0000	1.0000	1.0000	0.9998	0.9944	0.9675	0.9085	0.8215	0.7193	0.6160
36	1.0000	1.0000	1.0000	0.9999	0.9952	0.9710	0.9167	0.8351	0.7375	0.6369
38	1.0000	1.0000	1.0000	0.9999	0.9958	0.9741	0.9239	0.8472	0.7539	0.6563
40	1.0000	1.0000	1.0000	0.9999	0.9964	0.9767	0.9302	0.8581	0.7690	0.6743

3. Determination of required signal to scanning factor ratios for various slopes and slope changes. The signals relate to the probability of detection and the scanning factor influences the size of the obstacles.

4. Computation of the probability for detection of an edge if the reference directions of the laser rays are uniformly distributed over the slopes near an edge point.

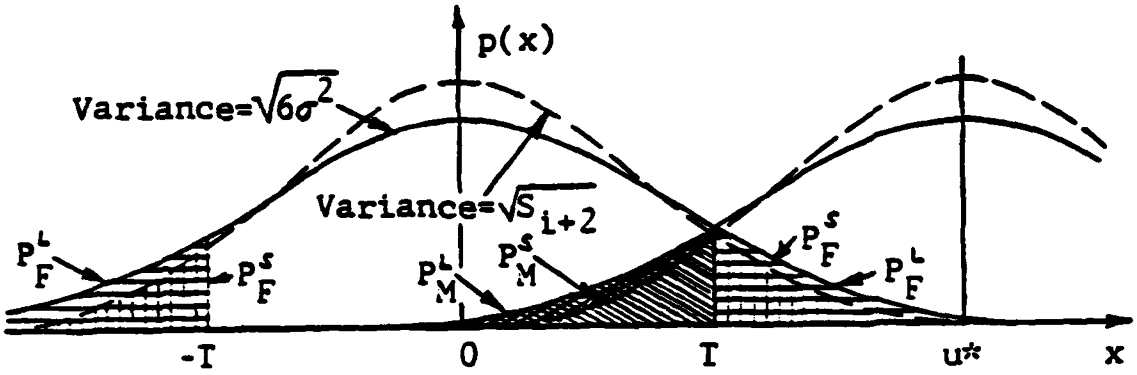

Figure 1. Distributions and Probabilities Comparing the Two Methods.

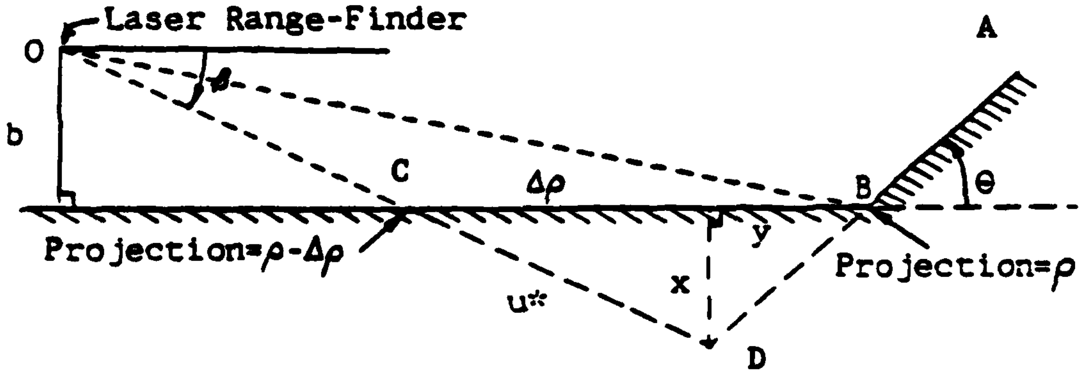

Figure 2. Obstacle Geometry

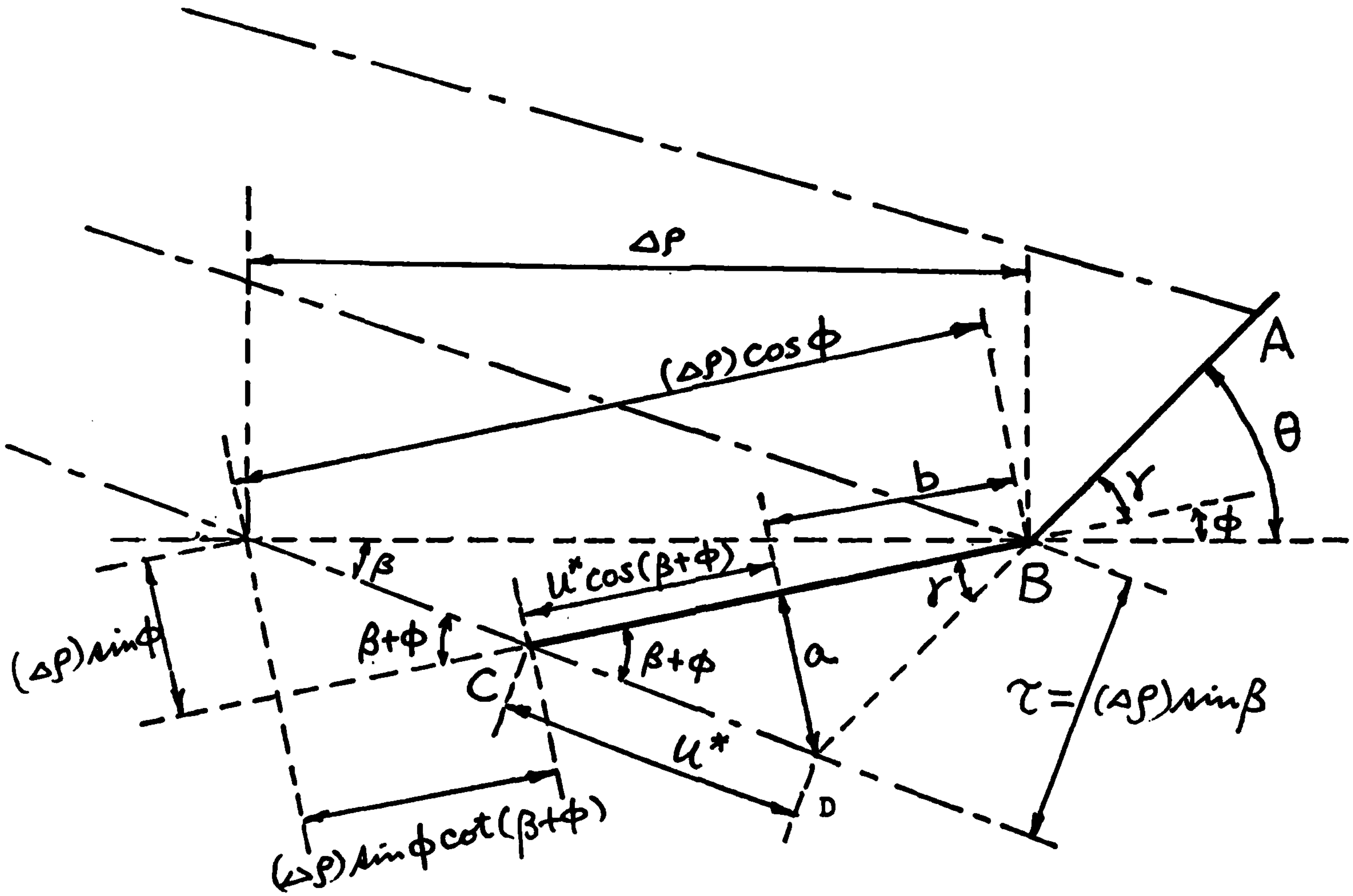

Figure 3. Angular Geometry

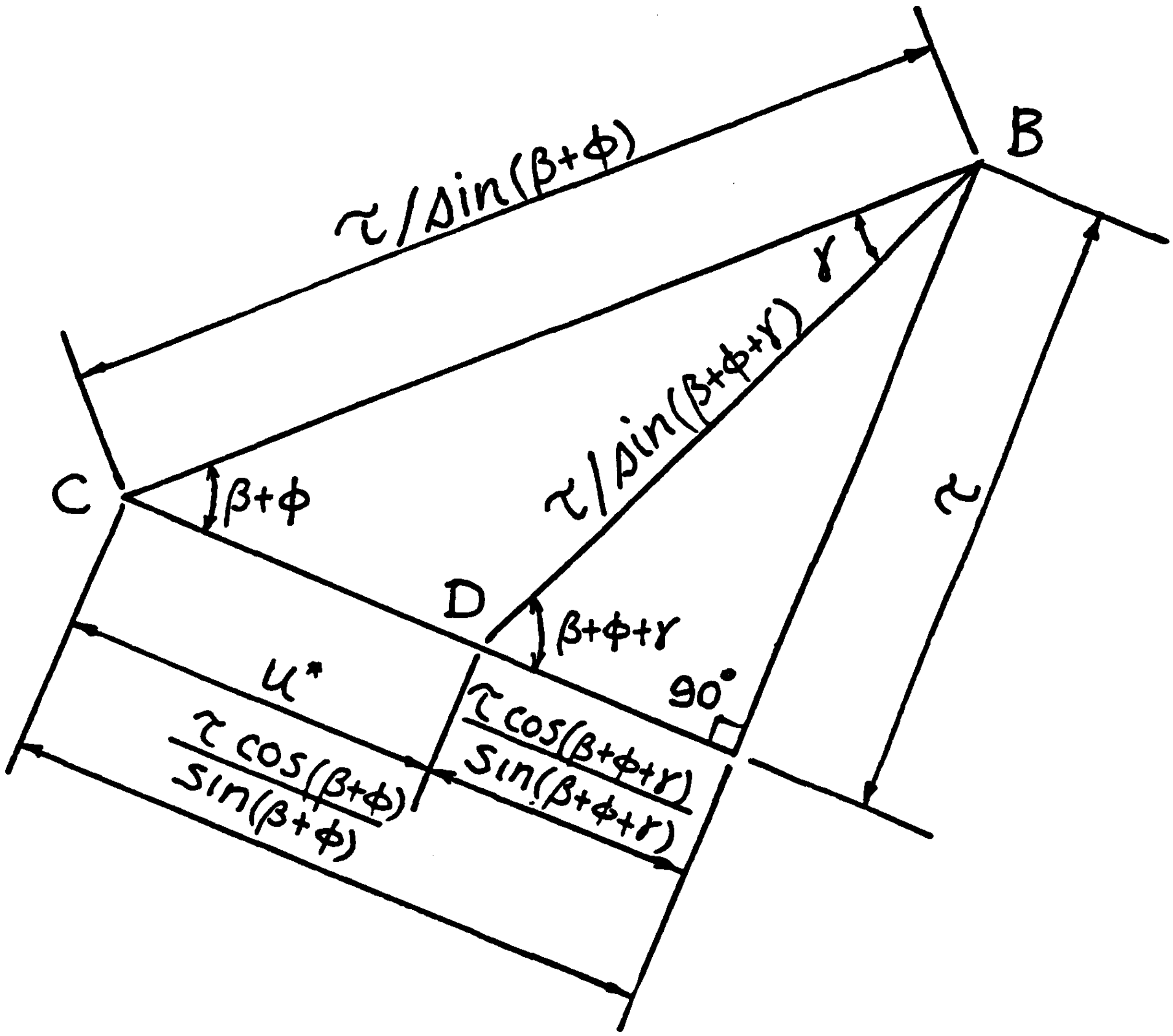

Figure 4. Projection Geometry

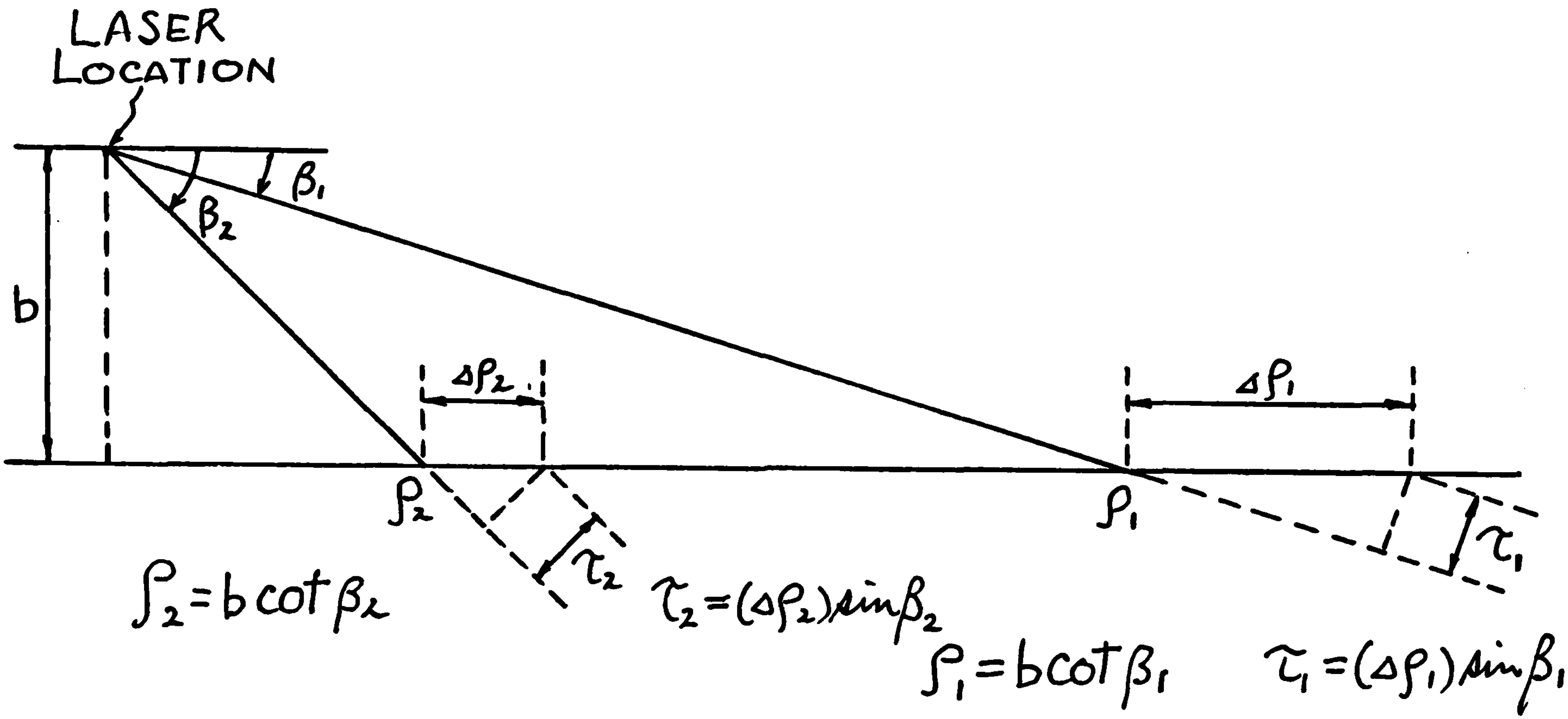

Figure 5. Scanning Factors

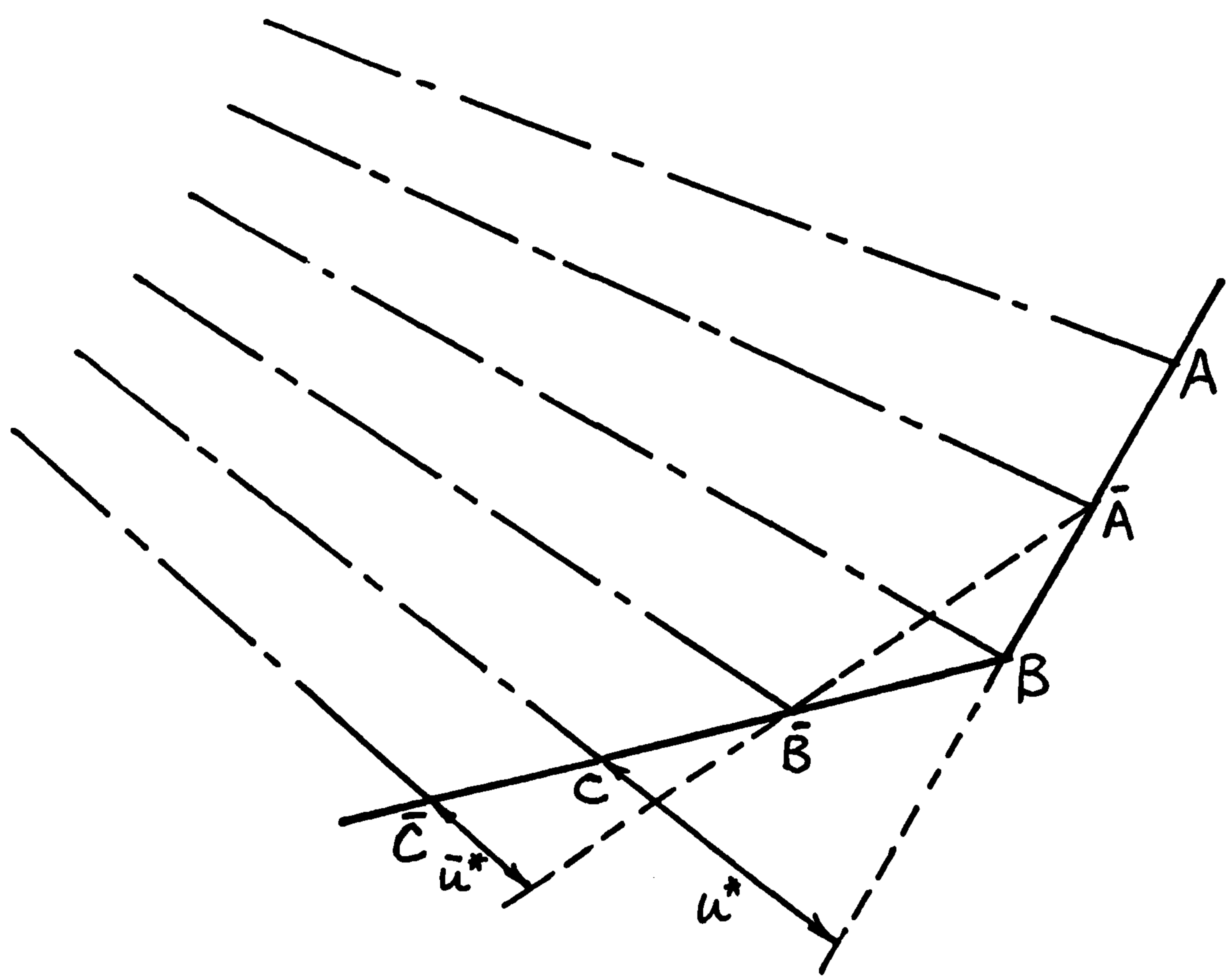

Figure 6. Reference Directions of Laser Rays Near an Edge Point

APPENDIX

THE SECOND RESIDUAL METHOD

The Second Residual Method, similar to the case with the Laplacian Method, considers cross-sections of terrain and looks for changes in slope. Here, however, a state estimation and decision process is used to perform the detection. A discrete second order linear time-varying system model is used to estimate ranges and gradients (slopes) from current and previous data. If the difference between a range measurement and range prediction is large enough, a change in slope is indicated and a special estimation scheme is employed.

THE SYSTEM MODEL

A stabilized system model for a terrain has been proposed. The state vector is

$$x_i = [d_i,\ g_i]^T \tag{A1}$$

where d_i indicates the i-th range and g_i the i-th gradient (or slope). A change of slope is modelled by the presence of an unknown input, u_i, which adds to the gradient component of x_i through the input matrix. The system model is

$$x_{i+1} = F_i x_i + Bu_i \tag{A2}$$

where

$$F_i = \begin{bmatrix} b_i & 1-c \\ 0 & q_i \end{bmatrix} \quad \text{and} \quad B = \begin{bmatrix} 0 \\ 1 \end{bmatrix}$$

where b_i and q_i are the time variant parameters and c is a small non-negative real number necessary for system stability while scanning inward from skylines. The measurement equation is

$$z_{i+1} = Hx_{i+1} + v_{i+1} \tag{A3}$$

where $H = [1,0]$ and v_{i+1} is zero mean Gaussian noise where

$$E\{v_i v_j\} = \begin{cases} 0 & \text{for all } i \neq j \\ \sigma^2 & \text{for all } i = j \end{cases} \tag{A4}$$

Our problem, then, is to detect any small nonzero inputs u_i, since they represent a change in slope.

As in the Laplacian Method, a sufficient statistic is necessary to detect the change of slopes. This sufficient statistic is called the residue, r_{i+2}, as

$$r_{i+2} = z_{i+2} - HF_{i+1}x^*_{i+1} \tag{A5}$$

where x^*_{i+1} is optimal estimate of x_{i+1} given $z_{i+1}, z_i, \ldots, z_1$. It can be shown that

$$\begin{aligned} E\{r_{i+1}\} &= HF_{i+1}Bu_i \\ &= (1-c)u_i \cong u_i \end{aligned} \tag{A6}$$

TECHNICAL REPORT INTERNAL DISTRIBUTION LIST

	NO. OF COPIES
CHIEF, DEVELOPMENT ENGINEERING BRANCH	
ATTN: SMCAR-CCB-D	1
-DA	1
-DP	1
-DR	1
-DS (SYSTEMS)	1
-DS (ICAS GROUP)	1
-DC	1
-DM	1
CHIEF, ENGINEERING SUPPORT BRANCH	
ATTN: SMCAR-CCB-S	1
-SE	1
CHIEF, RESEARCH BRANCH	
ATTN: SMCAR-CCB-R	2
-R (ELLEN FOGARTY)	1
-RA	1
-RM	1
-RP	1
-RT	1
TECHNICAL LIBRARY	5
ATTN: SMCAR-CCB-TL	
TECHNICAL PUBLICATIONS & EDITING UNIT	2
ATTN: SMCAR-CCB-TL	
DIRECTOR, OPERATIONS DIRECTORATE	1
DIRECTOR, PROCUREMENT DIRECTORATE	1
DIRECTOR, PRODUCT ASSURANCE DIRECTORATE	1

NOTE: PLEASE NOTIFY DIRECTOR, BENET WEAPONS LABORATORY, ATTN: SMCAR-CCB-TL, OF ANY ADDRESS CHANGES.

TECHNICAL REPORT EXTERNAL DISTRIBUTION LIST

	NO. OF COPIES
ASST SEC OF THE ARMY RESEARCH & DEVELOPMENT ATTN: DEP FOR SCI & TECH THE PENTAGON WASHINGTON, D.C. 20315	1
COMMANDER DEFENSE TECHNICAL INFO CENTER ATTN: DTIC-DDA CAMERON STATION ALEXANDRIA, VA 22314	12
COMMANDER US ARMY MAT DEV & READ COMD ATTN: DRCDE-SG 5001 EISENHOWER AVE ALEXANDRIA, VA 22333	1
COMMANDER ARMAMENT RES & DEV CTR US ARMY AMCCOM ATTN: SMCAR-FS	1
SMCAR-FSA	1
SMCAR-FSM	1
SMCAR-FSS	1
SMCAR-AEE	1
SMCAR-AES	1
SMCAR-AET-O (PLASTECH)	1
SMCAR-MSI (STINFO) DOVER, NJ 07801	2
DIRECTOR BALLISTICS RESEARCH LABORATORY ATTN: AMXBR-TSB-S (STINFO) ABERDEEN PROVING GROUND, MD 21005	1
MATERIEL SYSTEMS ANALYSIS ACTV ATTN: DRXSY-MP ABERDEEN PROVING GROUND, MD 21005	1
COMMANDER US ARMY AMCCOM ATTN: SMCAR-ESP-L ROCK ISLAND, IL 61299	1
COMMANDER ROCK ISLAND ARSENAL ATTN: SMCRI-ENM (MAT SCI DIV) ROCK ISLAND, IL 61299	1
DIRECTOR US ARMY INDUSTRIAL BASE ENG ACTV ATTN: DRXIB-M ROCK ISLAND, IL 61299	1
COMMANDER US ARMY TANK-AUTMV R&D COMD ATTN: TECH LIB - DRSTA-TSL WARREN, MI 48090	1
COMMANDER US ARMY TANK-AUTMV COMD ATTN: DRSTA-RC WARREN, MI 48090	1
COMMANDER US MILITARY ACADEMY ATTN: CHMN, MECH ENGR DEPT WEST POINT, NY 10996	1
US ARMY MISSILE COMD REDSTONE SCIENTIFIC INFO CTR ATTN: DOCUMENTS SECT, BLDG. 4484 REDSTONE ARSENAL, AL 35898	2
COMMANDER US ARMY FGN SCIENCE & TECH CTR ATTN: DRXST-SD 220 7TH STREET, N.E. CHARLOTTESVILLE, VA 22901	1

NOTE: PLEASE NOTIFY COMMANDER, ARMAMENT RESEARCH AND DEVELOPMENT CENTER, US ARMY AMCCOM, ATTN: BENET WEAPONS LABORATORY, SMCAR-CCB-TL, WATERVLIET, NY 12189, OF ANY ADDRESS CHANGES.

TECHNICAL REPORT EXTERNAL DISTRIBUTION LIST (CONT'D)

	NO. OF COPIES
COMMANDER US ARMY LABCOM MATERIALS TECHNOLOGY LAB ATTN: SLCMT-IML WATERTOWN, MA 01272	2
COMMANDER US ARMY RESEARCH OFFICE ATTN: CHIEF, IPO P.O. BOX 12211 RESEARCH TRIANGLE PARK, NC 27709	1
COMMANDER US ARMY HARRY DIAMOND LAB ATTN: TECH LIB 2800 POWDER MILL ROAD ADELPHIA, MD 20783	1
COMMANDER NAVAL SURFACE WEAPONS CTR ATTN: TECHNICAL LIBRARY CODE X212 DAHLGREN, VA 22448	1
DIRECTOR US NAVAL RESEARCH LAB ATTN: DIR, MECH DIV CODE 26-27, (DOC LIB) WASHINGTON, D.C. 20375	1 1
COMMANDER AIR FORCE ARMAMENT LABORATORY ATTN: AFATL/DLJ AFATL/DLJG EGLIN AFB, FL 32542	1 1
METALS & CERAMICS INFO CTR BATTELLE COLUMBUS LAB 505 KING AVENUE COLUMBUS, OH 43201	1

NOTE: PLEASE NOTIFY COMMANDER, ARMAMENT RESEARCH AND DEVELOPMENT CENTER, US ARMY AMCCOM, ATTN: BENET WEAPONS LABORATORY, SMCAR-CCB-TL, WATERVLIET, NY 12189, OF ANY ADDRESS CHANGES.

END

DTIC

5-86